K. Bartova – M. Domankova – J. Janovec *

INFLUENCE OF SECONDARY PHASE PRECIPITATION ON RESISTANCE TO INTERGRANULAR CORROSION OF AISI 316L AUSTENITIC STAINLESS STEEL

The AISI 316L steel after cold working of 40% and subsequent annealing at 750°C for 1, 2, 5, 10, 50, or 100 h was investigated. For the microstructure characterization the light microscopy and the transmission electron microscopy were used. To determine the sensitivity to intergranular corrosion the test was performed according to ASTM A 262, practice A. The transition between non-sensitised and sensitised states was found to be between 1 and 2 h of annealing. Sigma, laves and chi phases were identified in all the analyzed conditions. $M_{23}C_6$ was found to start to precipitate between 5 and 10 h of annealing. Sigma, chi, and $M_{23}C_6$ precipitated mainly along the grain boundaries. Laves precipitated mainly inside the grains, and after 50 h of annealing also intergranularly. Time dependent changes in the average metal composition of particular phases were considered as negligible.

Key words: austenitic stainless steel, intergranular corrosion, secondary phase precipitation, transmission electron microscopy

1 Introduction

Austenitic stainless steels (ASS) are frequently used as construction materials of various components in chemical, petrochemical, pharmaceutical and nuclear power industries, because of their excellent corrosion resistance and good mechanical properties at elevated temperatures [1–4]. However, properties of these steels depend strongly on structural, compositional, and morphological characteristics of the grain boundaries, e.g. on the state of intergranular precipitation [5–7].

On heat treatment, welding or service, the unstabilized ASS can be sensitised if isothermally exposed at temperatures 500–800°C or slowly cooled through this temperature range [1, 4, 8, 9]. The sensitisation resulting from microstructural changes can cause intergranular corrosion of unstabilized ASS. The microstructural changes evoking the sensitisation reside mostly in the precipitation of secondary chromium-rich phases (e.g. $M_{23}C_6$, sigma, chi) along the grain boundaries followed by the formation of chromium-depleted zones with chromium content below 12 wt% [10].

Sigma, as a typical phase occurring in the 316L steel, precipitates at temperatures between 550–900°C on grain boundaries, especially on triple points, incoherent twin boundaries and intergranular inclusions [11]. The sigma precipitation has a very slow kinetics, so the formation of precipitates can take hundreds to thousands of hours. Cold work (CW) accelerates its precipitation particularly if also recrystallization occurs on subsequent annealing [11]. Chi is mostly a minor phase and it was found in the AISI 316L steel at temperatures about 750 °C [7]. The formation of this phase can be observed mainly on the grain boundaries, incoherent twin boundaries, coherent twin boundaries and on dislocations within the matrix. Owing to its ability to dissolve carbon and also to its easier nucleation, the chi precipitation, when it occurs, precedes the sigma formation. The chi nucleation is also accelerated by cold work [11]. Laves of the Fe_2Mo type was found in AISI 316 steels with the bulk Mo content between 2–3 wt.% after long-term annealing. It is often a minor phase precipitating intragranularly in the form of equiaxed particles, with occasional occurrence at the grain boundaries [11].

The degree of sensitisation is influenced by many factors, e.g. bulk composition of the steel, grain size, plastic deformation, time-temperature exposure [1, 2, 4, 7]. The influence of time-temperature exposure on the steel sensitisation can be derived from time-temperature-sensitisation (TTS) diagram. In the diagram, each condition characterized by time and temperature of annealing is assigned to the sensitised or the non-sensitised areas separated by typical C-curve. The nose of this curve defines the critical temperature with the minimal time for sensitisation.

In the present work the AISI 316L steel was investigated. The aim of the study resides in the determination of relationships between the steel thermal-deformation history, its resistance to intergranular corrosion, and the state of precipitation. The attention was paid to the characterization of type, metal composition, amount, and distribution of secondary phase particles.

* **K. Bartova[1], M. Domankova[2], J. Janovec[3]**
[1] Institute of Materials Science, Faculty of Materials Science and Technology in Trnava,
[2] Slovak University of Technology in Bratislava, Slovakia, E-mail.: katarina.bartova@stuba.sk

2. Experimental procedure

The chemical composition of the investigated AISI 316L steel is given in Table 1. In the first step, the steel was solution annealed for 1h at 1100 °C. Immediately after the solution annealing, the steel was water quenched to eliminate the formation of new precipitates. In the second step, cold working of the steel sheets was applied at ambient temperature with the deformation of 40 % toward the original sheet thickness. The final step of the sample treatment resided in the isothermal annealing performed at 750 °C for 1, 2, 5, 10, 50 and 100 h.

The samples for the light microscopy were polished up to fine diamond finish (~1μm) and then electrolytically etched for 10–30 s (in dependence on the sample sensitisation) using 10 % oxalic acid at the current density 1 $A.cm^{-2.}$ The metallographic sections were observed by a light microscope NEOPHOT 32 equipped with CCD camera. The samples were tested to determine the sensitivity to intergranular corrosion according to ASTM A 262, practice A (Oxalic Acid Etch Test). In the corrosion test, the same etching procedure as described above for preparing metallographic samples was used, except for the etching time taking 90 s. The following criterion was applied to classify the sensitivity of the etched microstructures to the intergranular corrosion:

- the step structure, when the grain boundaries are not attacked by corrosion,
- the dual structure, when the grains are not completely surrounded by deeply etched boundaries,
- the ditch structure, when at least one grain is completely surrounded by deeply etched boundaries.

The samples showing step or dual structures were considered to be non-sensitised, whereas the samples exhibiting the ditch structure were classified as sensitised [12].

For the identification of secondary phases the transmission electron microscopy (TEM) of extraction carbon replicas was utilised. TEM observations were performed using a JEOL 200 CX microscope operated at 200 kV. It was equipped with an energy dispersive

X-ray spectrometer (EDX). The samples for TEM were prepared as follows:

- etching of the mechanically polished surfaces for 2–3 min with etchant consisting of 10 ml H_2SO_4, 10 ml HNO_3, 20 ml HF and 50 ml H_2O,
- coating of the surfaces with a thin layer of carbon,
- removing the carbon film from the samples in 8 % solution of HCl in ethanol.

At least ten EDX analyses per secondary phase were performed for each condition. At the evaluation of EDX spectra the standardless method for thin specimens was used.

The phase equilibria were calculated for the system corresponding to the investigated steel in the temperature range 500–1500 °C by ThermoCalc software [13] using the database STEEL17 formulated by Kroupa et al. [14]. In the calculation procedure the total Gibbs energy of the system consisting of contributions of individual phases is minimized at constant temperature and pressure. The particular phases were modelled as a sum of the reference level of Gibbs energy, entropy term, excess Gibbs energy, and magnetic term (if plausible the magnetic ordering). In the calculations, the elements Fe, C, Si, Mn, Cr, Mo and Ni were considered, and the phases liquid, delta-ferrite (b.c.c.), austenite (f.c.c.), laves (h.c.p.), M_6C (f.c.c.), $M_{23}C_6$ (f.c.c.), sigma (tetragonal) and chi (b.c.c.) were taken into account.

3. Results

The microstructures of the investigated steels after the solution annealing are composed of polyhedral austenitic grains containing twins (Fig. 1a). After cold working the grains are prevailingly acicular and contain shear bands (Fig. 1b). No precipitates were observed at the grain boundaries of both solution annealed and cold worked conditions. Black discrete areas randomly distributed across the microstructure of the cold worked condition are probably etching artefacts.

TTS diagram for the AISI 316L steel after 40% cold working is illustrated in Fig. 2a. Circles represent experimental results after oxalic acid etch test for the conditions annealed at 750 °C. The solid circles represent sensitised conditions showing the ditch structure. The condition 750 °C/1 h exhibiting the dual structure is illustrated by the empty circle. The microstructures corresponding to conditions 750 °C/1 h and 750 °C/5 h are documented in Figs. 2b and 2c, respectively.

On annealing, secondary phases were observed to start to precipitate on the grain boundaries and in the grain interior. The phases identified are summarized in Table 2. Figs. 3a and 3b show the microstructures of the investigated steel after annealing at 750 °C for 1 h and 2 h, respectively. $M_{23}C_6$ (Fig. 4), chi (Fig. 5) and sigma (Fig. 6) were identified on grain boundaries. Moreover, the particles of laves (Fig. 7) were evidenced. In Figs. 4–7 both the analysed particles and the corresponding diffraction patterns are documented. Average metal compositions of identified secondary phases in the analysed conditions can be seen in Table 3.

Chemical composition of the investigated steel — Table 1

Steel	Contents of elements in wt.%										
	C	N	Si	Mn	P	S	Cr	Ni	Mo	Ti	Fe
AISI 316L	0.021	0.019	0.62	1.10	0.0027	0.004	17.47	12.20	2.10	-	bal.

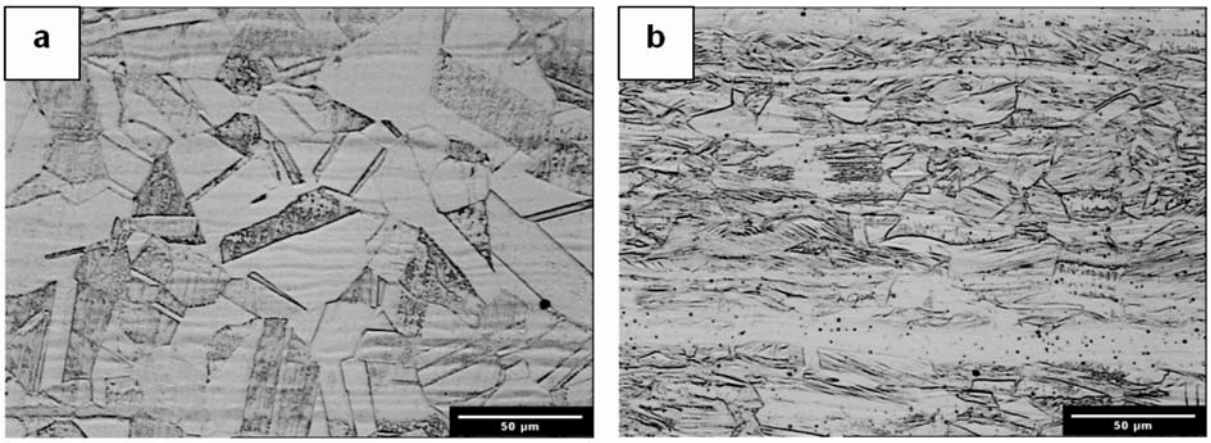

Fig. 1 Microstructures of the investigated steel after solution annealing (a) and subsequent 40 % cold work (b)

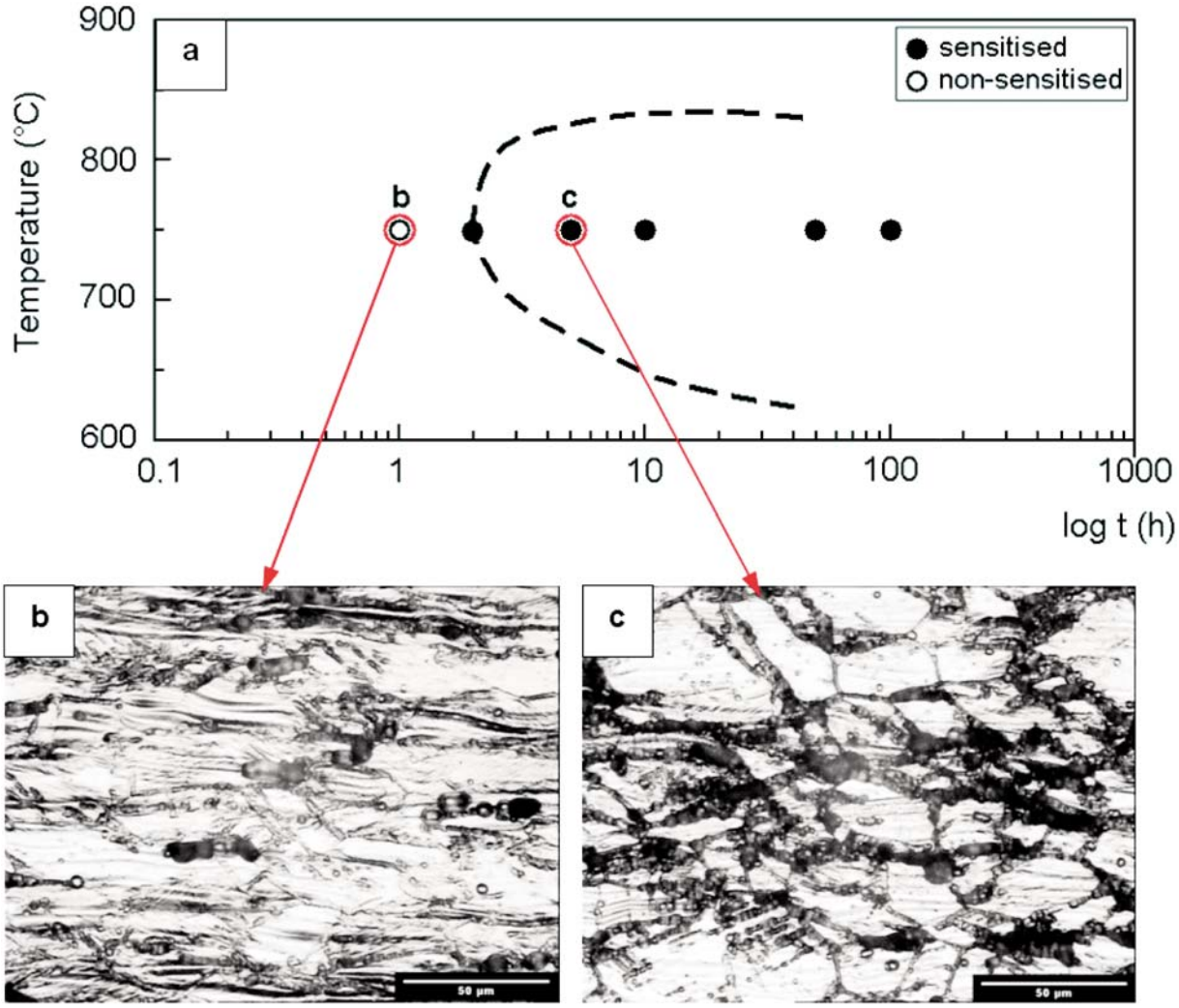

Fig. 2 TTS diagram for the AISI 316L steel after 40% cold working (the circles represent experimental results after oxalic acid etch test for conditions annealed at 750 °C) (a), the microstructure of condition 750 °C/1 h – dual structure (b), the microstructure of condition 750 °C/5 h – ditch structure (c)

Experimentally identified secondary phases in the investigated steel after 40% cold working and subsequent annealing at 750°C. Occurrence of a phase is denoted with symbol "X" Table 2

Annealing time (h)	Secondary phases			
	Sigma	Laves	Chi	$M_{23}C_6$
2	X	X	X	-
5	X	X	X	-
10	X	X	X	X
50	X	X	X	X
100	X	X	X	X

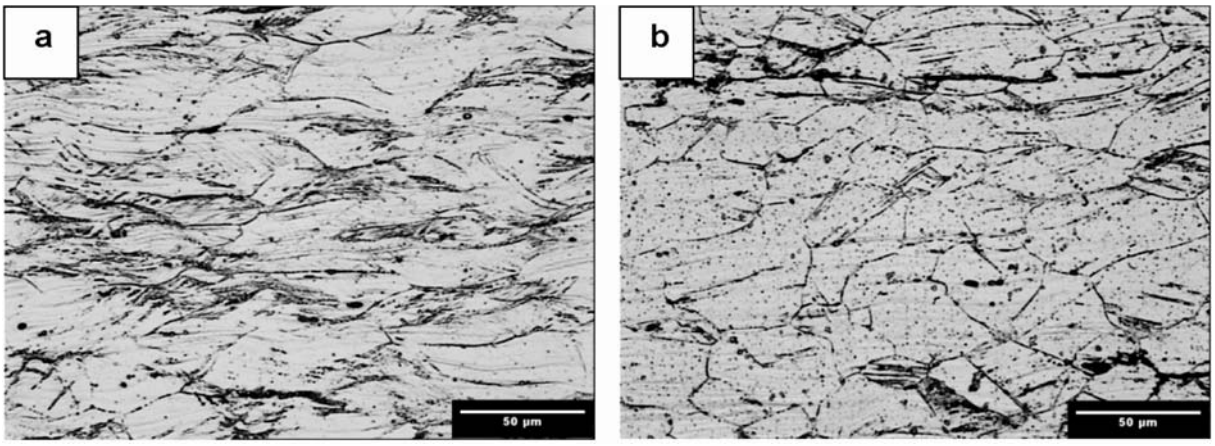

Fig. 3 Microstructures of the investigated steel after annealing at 750 °C/1 h (a), 750 °C/2 h (b)

Metal compositions of identified secondary phases in conditions annealed at 750 °C. Table 3
Average metal compositions of particular phases regardless of condition are highlighted (italic + bolt)

Secondary phases	Annealing time (h)	Mass contents of elements in %				
		Cr	Fe	Mo	Ni	Si
Sigma	2	33.0 ± 1.3	51.2 ± 2.6	10.6 ± 2.6	4.0 ± 0.6	1.3 ± 0.4
	5	32.9 ± 3.9	46.4 ± 4.8	12.9 ± 3.2	5.7 ± 2.7	2.0 ± 2.0
	10	32.7 ± 3.2	48.0 ± 4.8	11.9 ± 4.4	5.1 ± 2.5	2.3 ± 2.7
	50	31.9 ± 2.5	47.8 ± 1.1	13.5 ± 2.7	5.0 ± 0.6	1.9 ± 0.6
	100	32.7 ± 2.2	49.4 ± 2.8	11.3 ± 3.0	5.2 ± 1.2	1.5 ± 0.9
Average metal composition of sigma		32.6 ± 0.9	48.6 ± 3.6	12.0 ± 2.3	5.0 ± 1.2	1.8 ± 0.8
Laves	2	14.4 ± 4.2	28.6 ± 6.5	49.0 ± 8.3	3.8 ± 2.1	4.2 ± 4.0
	5	12.4 ± 5.5	24.7 ± 6.6	51.5 ± 7.0	5.8 ± 4.1	5.6 ± 5.5
	10	11.7 ± 3.6	27.1 ± 9.0	49.6 ± 9.5	4.8 ± 4.6	6.7 ± 5.7
	50	9.7 ± 1.4	25.9 ± 2.5	51.0 ± 2.9	5.0 ± 1.1	8.4 ± 4.4
	100	10.1 ± 1.7	29.5 ± 1.3	49.5 ± 2.0	5.1 ± 1.5	5.9 ± 2.7
Average metal composition of laves		11.7 ± 3.5	27.2 ± 3.3	50.1 ± 2.1	4.9 ± 1.4	6.2 ± 3.1
Chi	2	21.5 ± 4.3	39.1 ± 4.0	33.2 ± 7.3	3.4 ± 1.9	2.7 ± 1.2
	5	25.6 ± 1.0	44.3 ± 2.9	23.7 ± 3.0	4.1 ± 1.2	2.5 ± 0.2
	10	24.3 ± 4.4	43.4 ± 5.7	26.0 ± 5.6	4.1 ± 1.6	2.2 ± 1.8
	50	23.3 ± 1.8	41.6 ± 2.3	27.0 ± 2.5	4.6 ± 0.7	3.5 ± 1.4
	100	22.4 ± 3.3	45.1 ± 5.0	25.2 ± 5.8	4.7 ± 0.9	2.5 ± 2.2
Average metal composition of chi		23.4 ± 3.1	42.7 ± 4.3	27.0 ± 7.1	4.2 ± 0.9	2.7 ± 1.0

Secondary phases	Annealing time (h)	Mass contents of elements in %				
		Cr	Fe	Mo	Ni	Si
$M_{23}C_6$	10	65.9 ± 0.9	15.0 ± 0.2	16.0 ± 0.9	2.9 ± 0.2	0.3 ± 0.0
	50	66.6 ± 5.5	13.7 ± 2.6	16.0 ± 4.5	3.2 ± 1.1	0.6 ± 1.0
	100	68.6 ± 2.3	13.6 ± 0.4	13.7 ± 2.0	3.5 ± 0.4	0.7 ± 0.3
Average metal composition of $M_{23}C_6$		67.0 ± 1.5	14.1 ± 1.0	15.2 ± 1.4	3.2 ± 0.3	0.5 ± 0.3

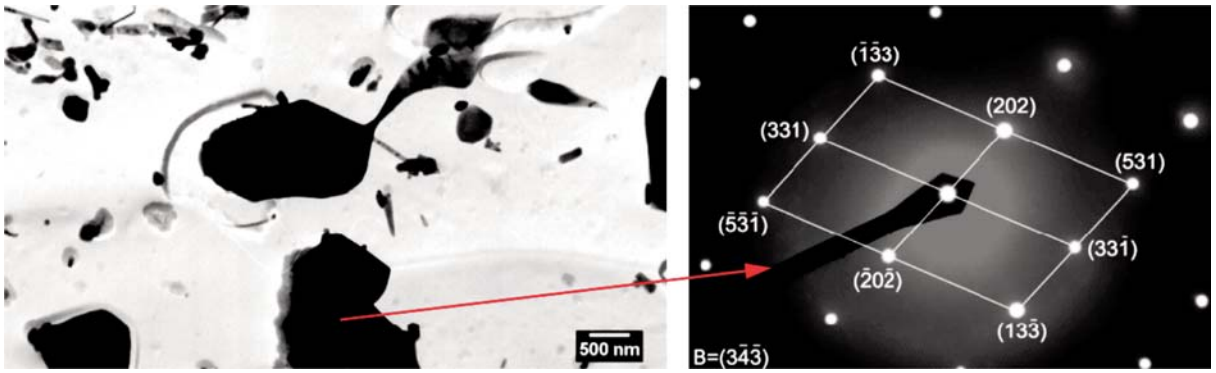

Fig. 4 Particle identified as M23C6 in the condition 750°C/100 h (a), diffraction pattern corresponding to the marked particle (b), TEM of carbon extraction replicas

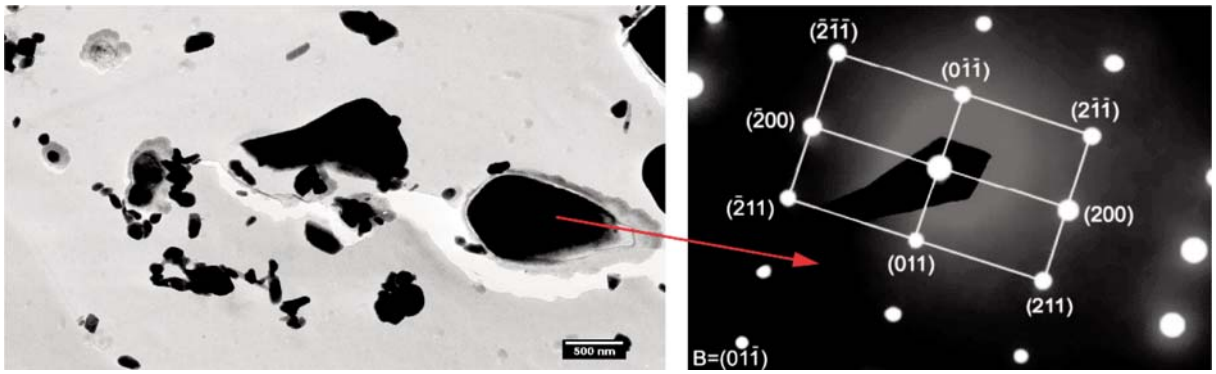

Fig. 5 Particle identified as chi in the condition 750°C/100 h (a), diffraction pattern corresponding to the marked particle (b), TEM of carbon extraction replicas

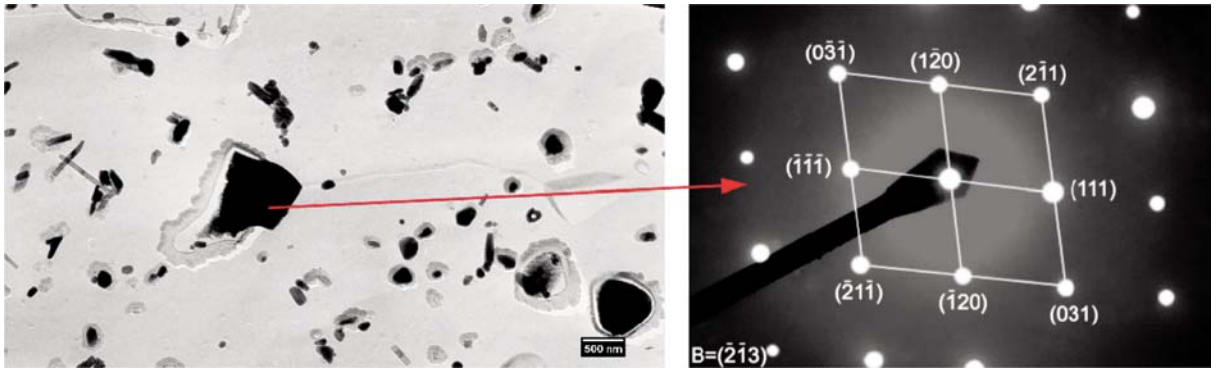

Fig. 6 Particle identified as sigma in the condition 750 °C / 100 h (a), diffraction pattern corresponding to the marked particle (b), TEM of carbon extraction replicas

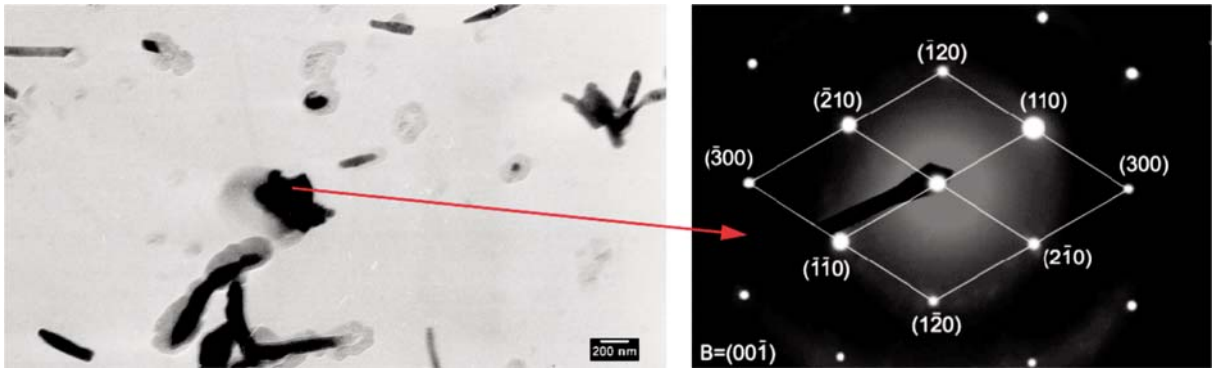

Fig. 7 Particle identified as laves in the condition 750°C/100 h (a), diffraction pattern corresponding to the marked particle (b), TEM of carbon extraction replicas

The experimental characterization of secondary phases was done for the sensitised conditions only. The results of the thermodynamic calculations performed for the temperature range 500–1500 °C are shown in Table 4. According to the prediction, $M_{23}C_6$ is the only secondary phase in equilibrium with austenite at 750 °C.

Phase equilibria predicted for the system corresponding to the investigated AISI 316L steel using ThermoCalc software — Table 4

Temperature range [°C]	Secondary phases predicted to be in equilibrium with austenite
500 – 657	$M_{23}C_6$ + M_6C + sigma
658 – 744	$M_{23}C_6$ + sigma
745 – 849	$M_{23}C_6$
850 – 1500	-

4. Discussion

Two important transitions between the analysed conditions of the AISI 316L steel were found as a result of the current study.

The transition between non-sensitised and sensitised states was determined between 1 and 2 h of annealing at 750 °C according to the corrosion test ASTM A 262, practice A (Fig. 2). During the annealing for 1 h (Fig. 3a) only small changes appear in the microstructure compared to the original 40% CW condition (Fig. 1b). In spite of the "acicular" microstructures documented in Figs. 1b and 3a, the microstructure of the condition annealed for 2 h (Fig. 3b) contains also polyhedral grains surrounded with intergranular particles both features typical for recrystallization. Thus, it is probable that the sensitisation starts between 1 and 2 h of annealing due to a progress in the microstructure recovery and recrystallization.

The another important transition observed between 5 and 10 h of annealing concerns the number of identified secondary phases in the analysed conditions (Table 2). In general, the amount of secondary phase particles in the microstructure was found to increase with increasing the annealing time [7, 8, 11]. Sigma, laves and chi phases were identified in all conditions analysed. The precipitation of $M_{23}C_6$ started however between 5–10 h of annealing. This transition did not influence the steel resistance to intergranular corrosion (Fig. 2), because of a small amount of $M_{23}C_6$ particles in the low-carbon steel (Table 1) and the presence of chromium also in earlier precipitated intermetallic phases (Table 3).

Sigma, chi, and $M_{23}C_6$ were found to precipitate mainly along the grain boundaries. On the other hand, laves precipitated in the grain interior in the form of fine mostly longitudinal particles (Fig. 7). This is in agreement with findings of Padilha and Rios [11]. After 50 h of annealing laves was also found on the grain boundaries in the form of massive particles.

Thermodynamic predictions of phase equilibria for the system corresponding to the AISI 316L steel showed partial agreement with the experimental results. According to the prediction, $M_{23}C_6$ is the only secondary phase co-existing with austenite in equilibrium at 750 °C (Table 4). It shows that sigma, chi, and laves identified experimentally are probably stable phases on annealing for shorter times. In the investigated steel the equilibrium at 750 °C is expected to be reached after annealing for times evidently exceeding 100 h. Then, the amount of the equilibrium $M_{23}C_6$ should increase at the expense of the non-equilibrium intermetallic phases.

The annealing time was not found to influence significantly average values of the metal composition of identified phases. This made possible to calculate the average metal compositions for particular phases regardless of the condition (Table 3). The biggest standard deviations were determined for laves, because the analysed particles of this phase were of smallest dimensions.

5. Conclusions

In the present work the influence of secondary phase precipitation on the resistance to intergranular corrosion of the 40 % cold work AISI 316L steel annealed at 750 °C for 1, 2, 5, 10, 50, and 100 h was investigated. Based on the experimental results the main findings can be summarized as follows:

1. The transition between non-sensitised and sensitised states was found to be between 1 and 2 h of annealing.
2. Sigma, laves, and chi were identified in all the analyzed conditions although they were not predicted to be equilibrium phases at 750 °C. $M_{23}C_6$, predicted to be in equilibrium with austenite at 750 °C, started to precipitate between 5 and 10 h of annealing.
3. Particles of sigma, chi, and $M_{23}C_6$ were observed mainly along the grain boundaries. Laves formed fine mostly longitudinal particles in the grain interior. After 50h of annealing this phase was also observed on the grain boundaries in the form of massive particles.
4. The annealing time was found to influence the average metal composition of the identified secondary phases slightly only.

Acknowledgement

The authors wish to thank to the Grant Agency of the Ministry of Education of the Slovak Republic and the Slovak Academy of Sciences (VEGA) for financial support under the contract No. 1/0126/08.

References

[1] PARVATHAVARTHINI, N, DAYAL, R.K.: Influence of Chemical Composition, Prior Deformation and Prolonged Thermal Aging on the Sensitization Characteristics of Austenitic Stainless Steels, *Journal of Nuclear Materials* 305, 2002, pp. 209–219.
[2] PARVATHAVARTHINI, N, DAYAL, R.K, GNANAMOORTHY, J.B.: Influence of Prior Deformation on Sensitization of AISI Type 316LN Stainless Steel, *Journal of Nuclear Materials* 208, 1994, pp. 209–219.
[3] MAGULA, V, LIAO, J, IKEUCHI, K, KURODA, T, KIKUCHI, Y, MATSUDA, F. New Aspects of Sensitization Behaviour in Recent 316 Type Austenitic Stainless Steels, *Trans. JWRI,* Vol. 25, 1996, pp. 49–58.
[4] ZAHUMENSKY, P, TULEJA, S, ORSZAGOVA, J, JANOVEC, J, SILADIOVA, V.: Corrosion Resistance of 18Cr-12Ni-2,5Mo Steel Annealed at 500-1050°C, *Corrosion Science 41,* 1999, pp. 1305–1322.
[5] DOMANKOVA, M, MAREK P, MORAVCIK, R.: Effect of Annealing at 650°C on Precipitation in Chosen Austenitic Stainless Steels, *Acta Metallurgica Slovaca,* 13, 2007, pp. 52–60.
[6] MAREK, P, DOMANKOVA, M.: Influence of 40% Deformation on Sensitisation Characteristic of 316 and 316L Austenitic Stainless Steels, *Acta Metallurgica Slovaca*, 13, 2007, 61–67.
[7] VACH, M., KUNIKOVA, T., DOMANKOVA, M., SVEC, P., CAPLOVIC, L., GOGOLA, P., JANOVEC J.: Evolution of Secondary Phases in Austenitic Stainless Steels During Long-term Exposures at 600, 650, and 800°C, *Materials Characterization 59*, 2008, 1792–1798.
[8] WASNIK, D.N, DEY, G.K, KAIN, V, SAMAJDAR, I.: Precipitation Stages in a 316L Austenitic Stainless Steel, *Scripta Materialia*, 49, 2003, p. 135–141.
[9] AYDOGDU, G.H, AYDINOL, M.K.: Determination of Susceptibility to Intergranular Corrosion and Electrochemical Reactivation Behaviour of AISI 316L Type Stainless Steel, *Corrosion Science 48*, 2006, 3565–3583
[10] RAMIREZ, L.M, ALMANZA, E, MURR, L.E.: Effect of Uniaxial Deformation to 50% on the Sensitization Process in 316 Stainless Steel, *Materials Characterization 53*, 2004, 79–82
[11] PADILHA, A.F, RIOS, P.R.: Decomposition of Austenite in Austenitic Stainless Steels, *ISIJ International*, Vol. 42, 2002, No. 4, pp. 330–332.
[12] ASM Handbook Vol. 13A Corrosion: Fundamentals, Testing and Protection. *ASM International,* 2003, pp. 266-267.
[13] LUKAS, H.L., FRIES, S.G., SUNDMAN, B.: Computational Thermodynamics. The Calphad Method. *Cambridge University Press,* 2007.
[14] KROUPA, A.: *Personal Communication.*